DONNAN POTENTIALS FROM STRIATED MUSCLE LIQUID CRYSTALS

Sarcomere Length Dependence

ROBERT A. ALDOROTY, NIRA B. GARTY, AND ERNEST W. APRIL
Department of Anatomy and Cell Biology, College of Physicians and Surgeons of Columbia University, New York, New York 10032

ABSTRACT Donnan potentials from A-bands and I-bands were measured as a function of sarcomere length in skinned long-tonic muscle fibers of the crayfish. These measurements were made using standard electrophysiological technique. Simultaneously, the relative cross-sectional area of the fibers was determined. Lattice plane spacings and hence unit-cell volumes were determined by low-angle x-ray diffraction. At a sarcomere length at which the myosin filaments and actin filaments nominally do not overlap, measurements of potential, relative cross-sectional area, and unit-cell volume were used in conjunction with Donnan equilibrium theory to calculate the effective linear charge densities along the myosin filament ($6.6 \times 10^4\ e^-/\mu$) and actin filament ($6.8 \times 10^3\ e^-/\mu$). Using these linear charge densities, unit-cell volumes and Donnan equilibrium theory, an algorithm was developed to predict A-band and I-band potentials at any sarcomere length. Over the range of sarcomere lengths investigated, the predicted values coincide with the experimental data. The ability of the model to predict the data demonstrates the applicability of Donnan equilibrium theory to measurements of electrochemical potential from liquid-crystalline systems.

INTRODUCTION

It has been shown that potentials can be measured from the A-bands and I-bands of crayfish long-tonic fibers in the relaxed condition with the sarcolemma and internal membranes removed (Aldoroty and April, 1984). Measurements of potential have been reported for other gel and resin systems (Davis, 1942, 1945; Adair and Adair, 1934*a, b*, 1935) and for skeletal muscle cells in which the cell membrane has been disrupted (Aldoroty and April, 1981, 1982, 1984; Bartels and Elliott, 1981*a, b*, 1982; Elliott et al., 1978; Stephenson et al., 1981; Dewey et al., 1982; Bartels et al., 1980; Hinke, 1980; Scordalis et al., 1975; Pemrick and Edwards, 1974; Collins and Edwards, 1971). It has been widely hypothesized that these electrochemical potentials are of Donnan origin. A Donnan potential can result from an equilibrium condition in which a charged structural component, e.g., a gel or resin, in one phase of a two-phase ionic system causes an unequal distribution of diffusable anions and cations between the phases (Overbeek, 1956). The A-band of striated muscle is a hexagonally packed smectic B_1 liquid crystal composed of myosin filaments (Fig. 1) (Hawkins and April, 1981, 1983*a, b*; April, 1975*a, b*, 1978; Elliott and Rome, 1969). The isoelectric point of crayfish myosin filaments is ~4.4 (April, 1978). The isoelectric point of the actin filament is ~5.2 (Szent-Gyorgyi, 1947; Yu et al., 1970). Therefore, at physiological pH and under the experimental conditions, the myosin and actin filaments each carry a net negative charge. Thus, the myosin filaments of the A-band (a smectic B_1 liquid-crystalline lattice) and the actin filaments of the I-band (seemingly a type of nematic liquid crystal) provide the requisite charged structural components necessary to generate Donnan potentials. The following series of investigations considers the applicability of Donnan equilibrium theory to this experimental system.

Measurements of potential from A-bands and I-bands as a function of sarcomere length are reported. The degree of actin-filament interdigitation into the myosin-filament lattice is inversely proportional to the sarcomere length, and therefore can be decreased by stretching along the *c* axis. The electrochemical measurements of A-band and I-band potential were made concomitantly with light-microscopic measurements of fiber diameter that were transformed into relative fiber areas. Relative fiber areas correlate with relative unit-cell volumes obtained by low-angle x-ray diffraction (Hawkins and April, 1981, 1983*a*). With the above information, it is possible to test the applicability of Donnan equilibrium theory.

The unit-cell volume and amount of interdigitation between the charged myosin filaments and actin filaments

Dr. Aldoroty's present address is the Department of Surgery, Mount Sinai Medical Center, New York, NY.
Dr. Garty's present address is the Department of Hormone Research, Weizmann Institute of Science, Rehovot, Israel.

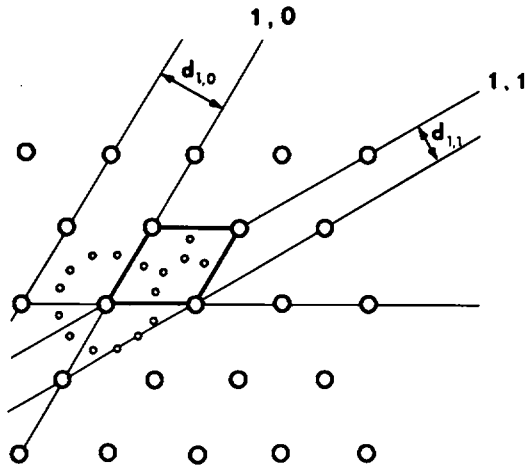

FIGURE 1 A schematic representation of a cross section of the myosin-filament lattice is shown. The large open circles represent myosin filaments that are arranged hexagonally and form the 1, 0 and 1, 1 lattice planes as indicated by the solid lines. The distance between lattice planes is indicated by $d_{(1,0)}$ and $d_{(1,1)}$. The myosin filaments are ~4.5 μm long and 18 nm in diam. The small open circles represent the interdigitating actin filaments, 12 of which are arranged equidistantly around each myosin filament, hence a 6:1 unit-cell ratio. (The unit cell is the rhombus formed by the intersection of 1, 0 lattice planes.) The actual actin-filament lattice is imperfect; there is a ratio of actin filaments/myosin filaments of 5.1:1 (see Analysis section). The actin filaments are ~3.6 μm long and 8 nm in diam. In crayfish muscle in the relaxed state the myosin and actin filaments are suspended in an aqueous ionic medium. In this particular muscle there are no apparent interconnecting structural components to which this arrangement may be attributed (April and Wong, 1976; April, 1969).

varies as a function of sarcomere length (April and Wong, 1976). Therefore, perturbing the sarcomere length should affect the measured potentials in a predictable manner. At a sarcomere length of 11.9 μm there is practically no overlap between myosin filaments and actin filaments. Therefore, the measured potential from the A-band can be solely attributed to the charge on the myosin filaments, and the measured potential from the I-band can be solely attributed to the charge on the actin filaments. From these measurements, at a sarcomere length where the A-band and I-band are pure, Donnan equilibrium theory is applied to calculate the effective linear charge densities of the myosin filament and actin filament. An algorithm, which uses these effective linear charge densities, unit-cell volume, and sarcomere length to calculate the fixed-charge concentration in the unit cell, tests the hypothesis that the measured potentials are Donnan potentials. At the sarcomere lengths studied, the algorithm successfully predicts the measured electrochemical potentials. This is interpreted as evidence that Donnan equilibrium theory applies to the A-bands and I-bands of the long-tonic striated muscle fibers of crayfish.

METHODS AND MATERIALS

All experiments were performed on long-tonic fibers from the carpodite extensor muscle of crayfish (*Orconectes*). The dissections followed previously described methods (Aldoroty and April, 1984). Single muscle fibers, 100 to 200 μm in diam., were transferred from curstacean saline (van Harreveld, 1936) to a crustacean relaxing solution (Table I). After mechanical skinning, the fibers were immersed in 1.0 ml/dl Triton X-100 in crustacean relaxing solution for 30 min in order to remove internal membranous structures. Then they were thoroughly washed with crustacean relaxing solution.

All the experiments were performed with the fiber in the relaxed condition. The physiologic conditions necessary to maintain the relaxed condition have been determined (Kawai and Brandt, 1976). The relaxed condition was insured by the composition of the relaxing solution, which contained an excess of calcium-free Mg-ATP, and by frequent changes of relaxing solution; no experiment lasted beyond 6 h.

Measurements of Potential

The preparation was mounted on the stage of an inverted microscope (M2 Nikon, Inc., Instrument Div., Garden City, NY) equipped with polarizing optics. A magnification of 600 provided a clear view of the A-bands and I-bands (Aldoroty and April, 1984). The sarcomere length was adjusted with a micromanipulator and was monitored by light diffraction (He-Ne laser, 0.3 mW, λ = 0.6328 μm, Spectra-Physics Inc., Mountain View, CA) (April et al., 1971).

Measurements of potentials were made using 3 mol/l KCl-filled microelectrodes with outer tip diameters of 0.3–0.4 μm. These correlate with electrode resistances of 10–15 MΩ (Aldoroty and April, 1984). Electrode resistance was monitored by passing current through the electrode such that 1 mV was equivalent to 1 MΩ. All measurements were recorded with a chart recorder (2200 series with a medium gain DC preamplifier, 13-461510, Gould Inc., Instruments Div., Cleveland, OH). The entire apparatus was protected from random radio frequency by appropriate screening and grounding.

The question of the sampling properties of the microelectrode is a significant factor in the interpretation of these experimental results. The filament spacing is one order of magnitude less than the microelectrode tip diameter. Consequently, the electrode averages the electrostatic potentials resultant from the individual myosin filaments and actin filaments or some function of the electrostatic potential. It has been shown that for muscle the average potential between the filaments equals the Donnan potential (Elliott and Bartels, 1982). Further, beginning from the Poisson-Boltzmann equation and a protein matrix of low charge concentration (e.g., muscle at pH 7.0), it has been demonstrated that the result of electrostatic theory is similar to Donnan equilibrium theory (Naylor, 1982). Such analytic approaches have demonstrated the validity of using KCl-filled microelectrodes to measure potentials from protein matrices of low charge density (e.g., the myosin-filament lattice of muscle).

Since work cannot be obtained from a system that is in equilibrium, and since a Donnan potential is an equilibrium condition, a Donnan potential only can be measured using a salt bridge. This adds a necessary

TABLE I
PREPARATION OF RELAXING SOLUTION AT PH 7.4

Component	Concentrations
	mmol/l
Potassium propionate	173
Tris	5
$MgCl_2$	1.12
Na_2H_2ATP	2
H_4EGTA*	5

See Kawai and Brandt (1976).
*H_4EGTA is ethylene glycol-bis-(β-amino-ethyl ether) *N,N'*-tetraacetic acid.

element of irreversibility to the system by introducing a liquid-junction potential (Overbeek, 1956). When the equations for a liquid-junction potential are applied to a system for the measurement of a Donnan potential, and when assumptions of ideality are incorporated, the equation reduces to the ideal expression for a Donnan potential (Overbeek, 1956). The assumptions of ideality have been discussed and shown to be reasonable (Elliott and Bartels, 1982).

Measurements of Fiber Diameter

Fiber diameter was measured as a function of sarcomere length with a filar micrometer mounted in the optical system of the inverted microscope (Blinks, 1965). The magnification via this optical pathway was 200.

Measurements of Myosin-Filament Lattice Plane Spacing

X-ray diffraction measurements of the A-band, myosin filament, $d_{(1,0)}$ lattice plane spacing (Fig. 1) were made using previously detailed methods (April et al., 1971; April and Wong, 1976). The source was the Cu Kα peak from a microfocus rotating anode x-ray generator (GX 6; Elliot Equipment Corp., Borhamwood, England) operated at 35 kV and 22 mA. Fibers were mounted in a low-angle camera of modified Franks design (April et al., 1971) and the diffraction patterns were collected electronically with a one-dimensional position-sensitive detector (PSD 1000 Tennelec Inc., Oak Ridge, TN). Collection times were ~15 min. The patterns were analyzed by computer (MINC 11/23, Digital Equipment Corp., Marlboro, MA) with programs that were developed in this laboratory.

RESULTS

Measurements of Potential

Potentials were measured in both the A-band and I-band regions over a range of sarcomere lengths. The measured A-band and I-band potentials are plotted against sarcomere length in Fig. 2 and are summarized in Table II. The A-band potentials become more negative as the sarcomere length is increased. The I-band exhibits a similar increase, albeit more gradual.

Measurements of Fiber Diameter

The measurements of fiber diameter were normalized to the fiber diameter at a sarcomere length of 9.7μm. The relationship between the relative fiber diameter and sarcomere length is shown in Fig. 3. A linear regression line describes the data (April and Wong, 1976).

Measurements of Myosin-Filament Lattice Plane Spacing

Low-angle x-ray diffraction of the crayfish fibers at a sarcomere length of 9.7 μm gave a mean myosin-filament interaxial spacing of 70 nm (SD = 3 nm). This spacing is equavilent to an A-band unit-cell volume of 1.9×10^{-14} cm^3. The unit-cell volume of the A-band myosin-filament lattice was calculated according to

$$V = l_m \frac{[d_{(1,0)}]^2}{\sin (60°)}, \qquad (1a)$$

where l_m represents the length of a myosin filament or

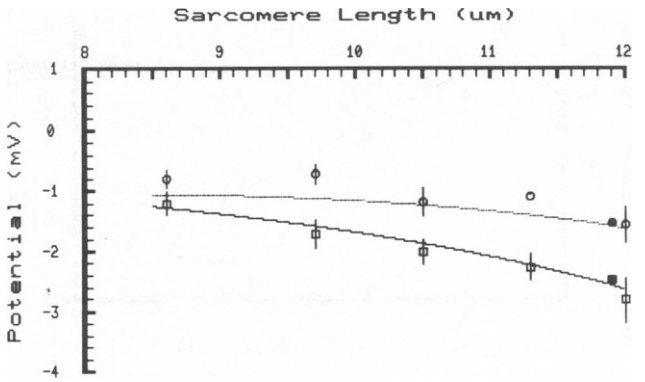

FIGURE 2 Potentials measured as a function of sarcomere length are shown. □ represents potentials measured from A-bands; o represents potentials measured from I-bands; bars indicate SD. The solid curves drawn are calculated from the algorithm described in the Analysis section. The *lower* curve represents the predictions of the algorithm for Donnan potentials from the A-band. The *upper* curve represents the predictions of the algorithm for Donnan potentials measured from the I-band. The ■ indicates the potential at a sarcomere length of 11.9 μm that corresponds to the myosin-filament linear charge density (6.6×10^4 e^-/μm) used to calculate the curve for the A-band. The ● indicates the potential at a sarcomere length of 11.9 μm that corresponds to the actin-filament linear charge density (6.8×10^3 e^-/μm) used to calculate the curves for the A-band and I-band.

A-band and $d_{(1,0)}$ is the lattice plane spacing (Fig. 1) (Hawkins and April, 1981). Interaxial myosin-filament spacings were calculated from

$$d_{(m,m)} = \frac{d_{(1,0)}}{\sin (60°)} \qquad (1b)$$

(April et al., 1971).

For this experimental system the relative unit-cell volumes obtained by low-angle x-ray diffraction measurements of lattice spacings are equivalent to relative fiber areas obtained from light microscopic measurements (Hawkins and April, 1981, 1983*a*). Since the length of a myosin filament is constant, it is possible to calculate absolute unit-cell volumes of the A-band from the correla-

TABLE II
RESULTS AND STATISTICS OF THE POTENTIAL MEASUREMENTS*

A-band				I-band		
L_s*	$\langle\psi_D\rangle$‡	SD§	n‖	$\langle\psi_D\rangle$	SD	n
μm	mV	mV		mV	mV	
8.6	−1.2	0.2	22	−0.8	0.2	15
9.7	−1.7	0.2	22	−0.7	0.2	11
10.5	−2.0	0.2	26	−1.2	0.2	35
11.3	−2.3	0.2	11	−1.1		1
12.0	−2.8	0.4	31	−1.6	0.3	20
12.5	−4.6	1.1	26	−2.1	0.5	4

*L_s is the sarcomere length.
‡$\langle\psi_D\rangle$ is the average measured potential.
§SD is the standard deviation of the measured potential.
‖n is the number of measurements of the potential.

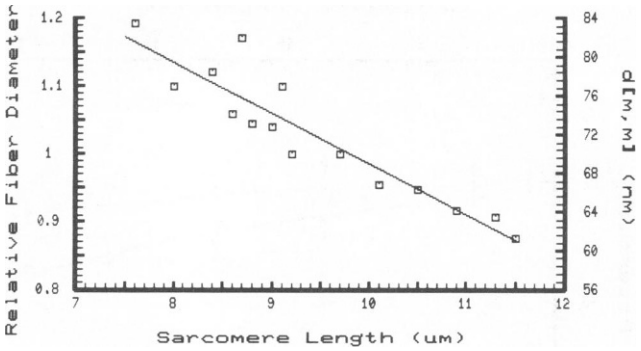

FIGURE 3 Relative cross-sectional areas of the muscle fibers measured as a function of sarcomere length are shown. The data points are derived from fiber diameter measurements that are normalized to the fiber diameter at a sarcomere length of 9.7 μm (50% myosin-filament/actin-filament overlap). Actual $d_{(m,m)}$ distances can be calculated from relative fiber diameter data given sufficient low-angle x-ray diffraction data. Skinned crayfish muscle has been shown to be nonisovolumetric with respect to sarcomere length (April and Wong, 1976). Hence, the data are plotted linearly. The linear regression constants are (*a*) Sarcomere length vs. relative fiber diameter: slope = $-0.075/\mu$m, *y*-intercept = 1.74, correlation coefficient = 0.9303, and $n = 15$; (*b*) sarcomere length vs. $d_{(m,m)}$: slope = -5.25 nm/μm, *y*-intercept = 121.3 nm, correlation coefficient = 0.9315, and $n = 15$.

tion between relative A-band areas and relative unit-cell volumes. The empirical expression is

$$V = \frac{A}{A_o} V_o, \tag{2}$$

where A/A_o is the relative fiber area and V_o is the unit-cell volume calculated from Eq. 1a. This equality is eminently reasonable because, without internal membranous structures, the sum of the unit-cell areas must equal the total fiber cross-sectional area. (The contribution by the sarcoplasmic reticulum has been removed by treating the fiber with the nonionic detergent, Triton X-100 [Aldoroty and April, 1984]). The relationship of both relative fiber diameter and interaxial spacing to sarcomere length is shown in Fig. 3.

ANALYSIS

According to Benedek and Villars (1979), the Donnan potential is

$$\psi_D = \frac{kT}{e} \ln\left\{\sqrt{1 + \frac{\Gamma^2}{4C^2}} - \frac{\Gamma}{2C}\right\}, \tag{3a}$$

where ψ_D is the Donnan potential; k is the Boltzmann constant; T is the temperature in degrees Kelvin; e is the charge on an electron; C is the concentration of mobile ions in the external phase; Γ is the fixed charge concentration due to protein (contractile filaments).

In turn

$$\Gamma = zC_z, \tag{3b}$$

where z is the unit charge on the protein with a concentration C_z. A derivation and discussion of this equation as it applies to this experimental system is presented in the Appendix. In keeping with previously published views, the A-band is treated as a single ionic phase (Hawkins and April, 1981, 1983*a*, *b*; April, 1978; Elliott, 1973). Further, the charges along the myosin filaments and actin filaments are assumed to be distributed evenly along the length of the filaments and in the plane perpendicular to the filaments. This assumption is reasonable considering the microenvironment that the microelectrode samples (Elliott and Bartels, 1982). Hence, it is possible to derive fixed charge concentrations (mol e^-/l) and effective linear charge densities (e^-/μm) for the unit cell. At a sarcomere length of 11.9 μm, there is nominally no overlap of the myosin filaments and actin filaments. Therefore, at this sarcomere length of 11.9 μm, the A-band potential can be considered the result only of the myosin filaments. The I-band potential is always the result only of the actin filaments. The filament concentration is given by

$$C_z = \frac{n}{NV}, \tag{3c}$$

where C_z is the myosin-filament or actin-filament concentration; n is the number of myosin or actin filaments per unit cell; N is Avogadro's number; and V is the unit-cell volume. From Eq. 3a, 3b and 3c the fixed charge concentration and the effective total charge on the myosin filaments and actin filaments can be calculated.

Calculation of the Myosin-Filament Effective Linear Charge Density at a Sarcomere Length of 11.9 μm

Under this condition the unit-cell volume is 1.4×10^{-14} cm^3. Applying Eq. 3c, where $n = 1$ myosin filament/unit cell, gives $C_z = 1.2 \times 10^{-7}$ mol myosin rod/l. Then Eq. 3a and 3b, where the A-band potential is -2.5 mV, yield 3.0×10^5 e^-/myosin filament or a linear charge density of 6.6×10^4 e^-/μm along the myosin filament.

Calculation of the Actin-Filament Effective Linear Charge Density at a Sarcomere Length of 11.9 μm

Under this condition an equivalent unit-cell volume is obtained for the I-band. A unit-cell area equal to the A-band unit-cell area is multiplied by the length of the actin filament. This yields an equivalent unit-cell volume of 1.1×10^{-14} cm^3. In the I-band the number of actin filaments per equivalent unit-cell is assumed to be six (an exact 6:1 unit-cell ratio). Applying Eq. 3c, where $n = 6$ actin filaments/equivalent unit cell, gives $C_z = 9.1 \times 10^{-7}$ mol actin filament/l. Then Eqs. 3a and 3b, where the I-band potential is -1.6 mV, yield 2.4×10^4 e^-/actin filament or a linear charge density of 6.8×10^3 e^-/μm along the actin filament.

At any sarcomere length, the A-band fixed charge concentration or the effective linear charge density of a unit cell can be reconstructed from the charge contributions of the myosin filaments and actin filaments. An algorithm was constructed to model the effects of changing sarcomere length on the measured potential. This model first calculates the half-length of an I-band and the full-length of a total overlap zone within the A-band

$$l_i = \frac{1}{2}(l_s - l_m - 2l_z) \tag{4a}$$

$$l_o = 2(l_a - l_i), \tag{4b}$$

where l_i is the half-length of an I-band; l_s is the length of a sarcomere; l_m is the length of a myosin filament (= 4.5 μm); l_z is the half-width of a Z-line (= 0.1 μm); l_o is the length of an overlap zone; and l_a is the length of an actin filament (= 3.6 μm). The A-band unit-cell volume at a given sarcomere length is computed using the linear regression constants given in the caption of Fig. 3 and Eqs. 1a and 1b. Then the filament concentration, C_z, is calculated according to Eq. 3c. It was determined that the A-band actin-filament lattice is incomplete (Hawkins and April, 1983*b*, Fig. 3, p. 246). The actual actin-filament/myosin-filament ratio is 5.1:1 (SD = 0.4 actin filaments).

The contributions of fixed charge concentration to the A-band unit cell from the myosin filament (subscript m) and actin filament (subscript a) are

$$\Gamma_m = z_m C_{zm}, \tag{5a}$$

where $z_m = l_m\,(6.6 \times 10^4\, e^-/\mu m)$ and

$$\Gamma_a = z_a C_{za}, \tag{5b}$$

where $z_a = l_o\,(6.8 \times 10^3\, e^-/\mu m)$. The total fixed charge concentration in the A-band unit-cell is

$$\Gamma_{total} = \Gamma_m + \Gamma_a. \tag{5c}$$

To this point the calculations have assumed that the electrode measures a Donnan potential from a single unit cell. This is not the case (Elliott and Bartels, 1982; Naylor, 1982). The volume sampled by the electrode must be constant. However, due to the nonconstant-volume relationship (April and Wong, 1976) the concentration of myosin filaments and actin filaments changes within the sampling volume in a predictable manner. Therefore, the Γ_{total} must be scaled such that

$$\Gamma_{effective} = \frac{\Gamma_{total}}{f}. \tag{5d}$$

At any sarcomere length this factor, f, is

$$f = \frac{V}{V_r} = \frac{(121.3 - 5.25L_s)^2}{(121.3 - 5.25L_{sr})^2}, \tag{5e}$$

where V is the unit-cell volume at the sarcomere length of interest, V_r is the reference unit-cell volume, and L_{sr} is the reference sarcomere length. The constants are obtained from a linear regression analysis (Fig. 3). In accordance with the nonconstant-volume relationship (April and Wong, 1976), V_r is chosen to be the unit-cell volume at a sarcomere length of 11.9 μm.

Finally, the model calculates a predicted Donnan potential from Eq. 3a. The same model is used to predict the measured I-band potentials. In this case, C_{za} is calculated assuming a ratio of 6:1 actin filaments/myosin filament, $C_{zm} = 0$ and $z_a = l_i\,(6.8 \times 10^3\, e^-/\mu m)$. The predictions for the A-bands and I-bands obtained from the model are plotted in Fig. 2. The predicted values coincide with the experimental data at the sarcomere lengths investigated.

DISCUSSION

Elliott (1973) suggested that the A-band of muscle may be regarded as a single phase, the dimensions of which are described by the volume of the myosin filaments, and that this phase should exhibit Donnan and osmotic properties in the absence of an enveloping membrane. Potentials were measured from the A-band and I-band at a sarcomere length (11.9 μm) at which there is nominally no myosin-filament/actin-filament overlap. From Donnan equilibrium theory, effective linear charge densities on the myosin filament and the actin filament in the relaxed condition are $6.6 \times 10^4\, e^-/\mu m$ and $6.8 \times 10^3\, e^-/\mu m$, respectively. These measurements agree closely with other estimates of linear charge density for the skinned crayfish fiber when only low-angle x-ray diffraction data are analyzed (April and Wong, 1976). Using the effective linear charge densities obtained in this series of experiments and the nonconstant volume behavior of skinned fibers (April and Wong, 1976), it was possible to construct a model that predicts the experimentally measured A-band potentials as a function of sarcomere length. Because the model generates good predictions of the experimental data (Fig. 2), it is concluded that, indeed, the microelectrode is measuring a Donnan potential generated by the myosin filaments and actin filaments that compose the A-band. The model also makes reasonable predictions for the I-band data (Fig. 2) and an analogous conclusion is drawn. Further, this model enables one to assess the individual contributions of the charge densities along the myosin filaments and actin filaments to the measured A-band potentials. The model demonstrates that, over the range of sarcomere lengths investigated, the myosin filaments are the major contributors to the measured A-band potentials and, therefore, dominate the shape of the sarcomere length/potential curve (Fig. 4).

The literature contains only one report of potentials measured as a function of sarcomere length from striated muscle in the relaxed condition with the sarcolemma disrupted (Pemrick and Edwards, 1974). In that experimental system (the glycerinated rabbit psoas muscle) the data ranged from −20 to −30 mV with a considerable amount of scatter, which might be due to the fact that

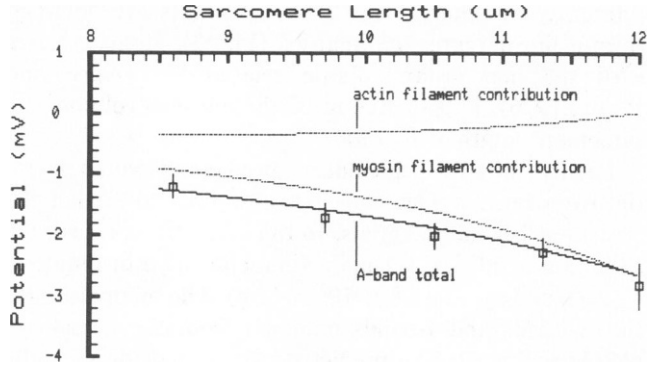

FIGURE 4 A-band potentials are plotted as a function of sarcomere length, demonstrating the contributions of the myosin filaments and actin filaments to the measured A-band potentials. The experimental data from the A-band have been plotted with SD bars. All curves were calculated using the algorithm described in the Analysis section. The *upper* curve shows the actin-filament contribution to the measured A-band potentials. The *middle* curve demonstrates the myosin-filament contribution to the measured A-band potentials. The *lower* curve, the sum of these contributions, represents the prediction of the model for the measured A-band potentials.

A-band and I-band impalements were not separated. They made no attempt to selectively impale A-bands and I-bands, a methodology that is well developed for the crayfish muscle (Aldoroty and April, 1981, 1982, 1984). Nevertheless, the sign of the slope of the least-squares line presented by Pemrick and Edwards (1974) is negative, which agrees with the crayfish data presented here. The difference between the absolute values of the Pemrick and Edwards data and those reported here may be attributable to species differences as well as the differing ionic strength and pH of the bathing media.

The measured A-band and I-band electrochemical potentials are predictable from myosin-filament and actin-filament linear charge densities; therefore, the Donnan equilibrium theory is applicable to this particular system. The data presented here support (*a*) the premise that the A-band of muscle may be regarded as a single Donnan phase (Elliott, 1973), and (*b*) the original concept that a Donnan potential can result from a charged structural component suspended in an ionic medium (Overbeek, 1956). It is reasonable to expect that the surface charges of the myosin filaments and the actin filaments would be the sources of an electrostatic repulsive force that has been implicated as one of the intermolecular forces stabilizing the A-band lattice (April, 1975*a*, 1978; Elliott and Rome, 1969).

APPENDIX

Derivation of an Expression for the Donnan Potential

Following the presentation of Benedek and Villars (1979), the activity coefficients are assumed equal and begin with the Nernst potential

$$\psi_i^n = -\frac{kT}{z_i e} \ln \frac{C_i(2)}{C_i(1)}, \tag{A1}$$

where ψ_i^n is the Nernst potential due to the ith ion; k is the Boltzmann constant; z_i is the valence on the ith ion; e is the charge on an electron; and $[C_i(2)/[C_i(1)]$ is the concentration ratio of the ith ion in compartments 1 and 2.

Limiting the conditions to monovalent ions, the conditions for bulk neutrality in each compartment are

$$\sum_i C_i^+(1) = \sum_i C_i^-(1) \tag{A2a}$$

$$\sum_i C_i^+(2) = \sum_i C_i^-(2) + \Gamma, \tag{A2b}$$

where the equivalent charge concentration of the fixed polyelectrolyte is Γ, which is equal to zC_z. The charge on the fixed polyelectrolyte is z and the concentration of the fixed polyelectrolyte is C_z.

Further, given the Gibbs-Donnan condition

$$\frac{C^+(1)}{C^+(2)} = \frac{C^-(2)}{C^-(1)}, \tag{A3}$$

one arrives at

$$\psi_D = \frac{kT}{2e} \ln \left\{ 1 - \frac{\Gamma}{\sum_i C_i^+(2)} \right\} \tag{A4a}$$

$$\psi_D = \frac{kT}{2e} \ln \left\{ \frac{\sum_i C_i^-(2)}{\sum_i C_i^+(2)} \right\}, \tag{A4b}$$

where $\psi_i = \psi_D = \psi_{\text{Donnan}}$ for all i. Finally, if

$$C(1) = \sum_i C_i^+(1) = \sum_i C_i^-(1), \tag{A5}$$

then

$$\psi_D = \frac{kT}{e} \ln \left\{ \sqrt{1 + \frac{\Gamma^2}{4C^2(1)}} - \frac{\Gamma}{2C(1)} \right\}. \tag{A6}$$

From the assumption of bulk electroneutrality, Eqs. A2a, A2b, and A4b, the Donnan potential results from the unequal distribution of diffusible anions and cations due to the presence of fixed charge in one of the phases.

Using Eq. A6, the behavior of the myosin-filament liquid-crystalline lattice with respect to the Donnan potential can be described. ψ_D is measured according to the methods outlined, while the right side of Eq. A6 contains the controlled variables. The system is such that the theoretical restrictions apply.

We thank Phillip W. Brandt and Masetaka Kawai (both of Columbia University, New York, NY) for the use of computer programs to calculate ionic concentrations and for reading the manuscript; Vincent F. Castellucci, Michael D. Gershon (both of Columbia University, New York, NY), and David W. Maughan (University of Vermont, Burlington, VT) for reading the manuscript.

This work was supported by the National Institutes of Health (5R01-AM15876) and the Equitable Life Assurance Society of the United States through the Insurance Medical Scientist Scholarship Fund.

Received for publication 5 January 1984 and in final form 5 July 1984.

REFERENCES

Adair, G. S., and M. E. Adair. 1934*a*. The determination of membrane potentials of protein solutions and the valence of protein ions. *Biochem. J.* 28:199–221.

Adair, G. S., and M. E. Adair. 1934*b*. The determination of the isoelectric and isotonic points of haemoglobin from measurements of membrane potentials. *Biochem. J.* 28:1230–1258.

Adair, G. S., and M. E. Adair. 1935. Methods and experimental technique. Part I (B). The determination of the electronic charge of colloidal ions. *Trans. Faraday Soc.* 31:130–135.

Aldoroty, R. A., and E. W. April. 1981. Microelectrode measurements of Donnan potentials within crayfish striated muscle. *J. Gen. Physiol.* 78:11*a*. (Abstr.)

Aldoroty, R. A., and E. W. April. 1982. Microelectrode measurement of A-band Donnan potentials as a function of relative volume. *Biophys. J.* 37 (2, Pt. 2):121*a*. (Abstr.)

Aldoroty, R. A., and E. W. April. 1984. Donnan potentials from striated muscle liquid crystals. A-band and I-band measurements. *Biophys. J.* 46:769–779.

April, E. W. 1969. The effects of tonicity and ionic strength on tension and filament lattice volume in single muscle fibers. Ph.D. thesis. Columbia University, New York, New York. 135 pp.

April, E. W. 1975*a*. Liquid crystalline characteristics of the thick filament lattice of striated muscle. *Nature (Lond.)*. 257:139–141.

April, E. W. 1975*b*. The myofilament lattice. Studies on isolated fibers IV. Lattice equilibria in striated muscle. *J. Mechanochem. Cell Motil.* 3:111–121.

April, E. W. 1978. Liquid cyrstalline contractile apparatus in striated muscle. ACS (Am. Chem. Soc.) Symp. Ser. No. 74. Mesomorphic Order in Polymers and Polymerization in Liquid Crystalline Media. 248–255.

April, E. W., P. W. Brandt, and G. F. Elliott. 1971. The myofilament lattice. Studies on isolated fibers. I. The constancy of the unit cell volume with variation in sarcomere length in a lattice in which the thin-to-thick myofilament ratio is 6:1. *J. Cell Biol.* 51:72–82.

April, E. W., and D. Wong. 1976. Non-isovolumic behavior of the unit cell of skinned striated muscle fibers. *J. Mol. Biol.* 101:107–114.

Bartels, E. M., T. D. Bridgman, and G. F. Elliott. 1980. A study of the electrical charges on the filaments in striated muscle. *J. Muscle Res. Cell. Motil.* 1:194. (Abstr.)

Bartels, E. M., and G. F. Elliott. 1981*a*. Donnan potentials from the A and I bands of skeletal muscle, relaxed and in rigor. *J. Physiol. (Lond.)*. 317:85P–86P.

Bartels, E. M., and G. F. Elliott. 1981*b*. Donnan potential measurements in A and the I band regions of barnacle muscle fibers under a variety of physiological conditions. *J. Gen. Physiol.* 78:12*a*. (Abstr.)

Bartels, E. M., and G. F. Elliott. 1982. Donnan potentials in rat muscle: differences between skinning and glycerination. *J. Physiol. (Lond.)*. 327:72P–73P.

Benedek, G. B., and F. M. H. Villars. 1979. Physics with Illustrative Examples of Medicine and Biology, Vol. 3. Electricity and Magnetism. Addison-Wesley Publishing Co., Inc. Reading, MA. 3-134–3-145.

Blinks, J. R. 1965. Influence of osmotic strength on cross-section and volume of isolated single muscle fibers. *J. Physiol. (Lond.)*. 177:42–59.

Collins, E. W., and C. Edwards. 1971. Role of Donnan equilibrium in the resting potentials in glycerol-extracted muscle. *Am. J. Physiol.* 221:1130–1133.

Davis, L. E. 1942. The significance of Donnan equilibria for soil colloidal systems. *Soil Sci.* 54:199–219.

Davis, L. E. 1945. A series of base-exchange equilibriums. *Soil Sci.* 59:379–395.

Dewey, M. M., S. F. Fan, and P. R. Brink. 1982. Measurement of Donnan potentials in relaxed and contracted muscle. *Biophys. J.* 37 (2, Pt. 2):125*a*. (Abstr.)

Elliott, G. F. 1973. Donnan and osmotic effects in muscle fibers without membranes. *J. Mechanochem. Cell Motil.* 2:83–89.

Elliott, G. F., and E. M. Bartels. 1982. Donnan potential measurements in extended hexagonal polyelectrolyte gels such as muscle. *Biophys. J.* 38:195–199.

Elliott, G. F., G. R. S. Naylor, and A. E. Woolgar. 1978. Measurements of the electric charge on the contractile proteins in glycerinated rabbit psoas using microelectrode and diffraction effects. *Ions in Macromolecular Biological Systems (Colston Papers. No. 29)*. 329–339.

Elliott, G. F., and E. M. Rome. 1969. Liquid cyrstalline aspects of muscle fibers. *Mol. Cryst. Liq. Cryst.* 5:647–650.

Hawkins, R. J., and E. W. April. 1981. X-ray measurements of the bulk modulus of the myofilament liquid crystal in striated muscle. *Mol. Cryst. Liq. Cryst.* 75:211–216.

Hawkins, R. J., and E. W. April. 1983*a*. The planar deformation behavior of skinned striated muscle fibers. *Mol. Cryst. Liq. Cryst.* 101:315–328.

Hawkins, R. J., and E. W. April. 1983*b*. Liquid crystals in living tissue. *Adv. Liq. Cryst.* 6:243–264.

Hinke, J. A. M. 1980. Water and electrolyte content of the myofilament phase in the chemically skinned barnacle fiber. *J. Gen. Physiol.* 75:531–551.

Kawai, M., and P. W. Brandt. 1976. Two rigor states in skinned crayfish single muscle fibers. *J. Gen. Physiol.* 68:267–280.

Naylor, G. R. S. 1982. On the average electrostatic potential between the filaments in striated muscle and its relation to a simple Donnan potential. *Biophys. J.* 38:201–204.

Overbeek, J. ThG. 1956. The Donnan equilibrium. *Prog. Biophys. Biophys. Chem.* 6:57–84.

Pemrick, S. M., and C. Edwards. 1974. Differences in the charge distribution of glycerol extracted muscle fibers in rigor, relaxation, and contraction. *J. Gen. Physiol.* 64:551–567.

Scordalis, S. P., H. Tedeschi, and C. Edwards. 1975. Donnan potential of rabbit skeletal muscle myofibrils. I. Electrofluorochromometric detection of potential. *Proc. Natl. Acad. Sci. USA*. 72:1325–1329.

Szent-Gyorgyi, A. 1947. Chemistry of Muscle Contraction. Academic Press, Inc., New York. 150 pp.

Stephenson, D. G., I. R. Wendt, and Q. G. Forrest. 1981. Non-uniform ion distributions and electrical potentials in sarcoplasmic regions of skeletal muscle fibers. *Nature (Lond.)*. 289:690–692.

van Harreveld, A. 1936. A physiologic solution for freshwater crustaceans. *Proc. Soc. Exp. Biol. Med.* 34:428–432.

Yu, L. C., R. M. Dowben, and K. Kornacker. 1970. The molecular mechanisms of force generation in striated muscle. *Proc. Natl. Acad. Sci. USA*. 66:1199–1205.